Mechanical behaviour of a prototype orthodontic retraction spring: a numerical–experimental study

M. A. Ferreira, R. Assumpção, M. A. Luersen and P. C. Borges
Department of Biomedical Engineering, Technical Federal University of Parana, Brazil

Correspondence to: M. A. Ferreira, 1183 Prefeito Omar Sabbag Avenue, Parana 80210-000, Brazil.
E-mail: regunteriato@yahoo.com.br

SUMMARY The purpose of this study was to examine the mechanical behaviour of orthodontic delta retraction springs. Twelve titanium–molybdenum (0.016 × 0.022 inch) delta loops were studied. The springs were analysed by means of the finite element (FE) method and experimental tests using a platform transducer. Each spring was activated from 0 to 6 mm. Statistical analysis of the data was carried out by one-way analysis of variance and Games–Howell parametric multiple comparison test for heterogeneous variances.

FE analysis revealed that the stress level varied from 277 to 1273 MPa. At 6.1 mm (773 MPa), the springs were still in the elastic range. Force levels varied from 0.1 N (10 g) to 2.2 N (224 g) at 1.4–8.1 mm of activation for the numerical study and from 0.44 N (45 g) at 1 mm to 2.02 N (206 g) at 6 mm of activation in the experimental study. The spring rate was within the levels that are appropriate for clinical use (34 g/mm). Vertical forces (F_y) showed constancy and were of low magnitude. The anterior moment/force ratio from the experimental tests was 14 at 3 mm of activation decreasing to 10.7, 8.7, and 7.2, for 4, 5, and 6 mm of activation, respectively. The springs could be activated up to 7 mm without exceeding the elastic limit.

Introduction

Sectional springs can be used to retract canines (Yang and Baldwin, 1974; Bourauel *et al.*, 1997) as well as to act as part of a segmented arch (Burstone, 1966, 1982; Manhartsberger *et al.*, 1989; Rinaldi and Johnson, 1995; Ferreira *et al.*, 2005) that retracts the anterior segment, the posterior segment, or both at the same time, depending on the treatment plan (alpha and beta moments and loop position will determine the type of tooth movement). The effectiveness of a spring is related to its geometry and the nature of the wire material (Burstone *et al.*, 1961; Yang and Baldwin, 1974; Ferreira, 1999). Springs must work within an elastic limit, should not harm the adjacent tissues, and should have a force system capable of producing controlled movement of one or more teeth. Alloys which are less resistant to deflection might be displaced more widely, without plastic deformation, and this is a characteristic of non-linear systems (Koenig *et al.*, 1980; Koenig and Burstone, 1989). Among the mechanical properties that characterize spring behaviour, spring rate plays a major role, for it allows the clinician to know its load deflection rate (Yang and Baldwin, 1974; Burstone, 1982).

The resulting stress from retraction spring activation lead to considerations about its elastic range, that is, how far a spring may be activated without surpassing the yield strength (YS) considering that once it is attained, it will no longer respond satisfactorily. Force systems resulting from retraction springs produce forces and moments that

determine the type of tooth movement, but springs with complex designs are not completely isometric and can become inaccurate for long activations (more than 3 or 4 mm). These force systems originating from orthodontic appliances have been studied experimentally (Solonche *et al.*, 1977; Vanderby *et al.*, 1977; Kum *et al.*, 2004), numerically (Yang and Baldwin, 1974; Haskell *et al.*, 1990; Raboud *et al.*, 1997; Siatkowski, 1997; Coimbra *et al.*, 2008), and with dynamic systems (Rhee *et al.*, 1997) or three-dimensional scanning systems to analyse movement of rigid bodies (Rhee *et al.*, 2002). The finite element (FE) method is used to simulate the behaviour of a body submitted to maximum stress. In this way, the influence of basic geometric parameters on a force system might if necessary be altered. In experimental methods, the body of evidence is submitted to mechanical tests, which might determine the force system more accurately.

A few studies have reported the stress along the spring body (Ferreira *et al.*, 2004; Coimbra *et al.*, 2008). Different types of load cells for measuring forces and moments have been described (Solonche *et al.*, 1977; Ferreira, 1999; Chen *et al.*, 2000; Ferreira *et al.*, 2005; Thiesen *et al.*, 2005) concerning orthodontic springs where the samples are submitted to tension, bending, and torsion testing at one or both sides of the spring to determine the force generated. A number of load cells have been developed to measure the degree of torsion (around the x, y, and z axes) at the extremities of the spring after activation (Ødegaard *et al.*,

1996; Torstein *et al.*, 1998; Kum *et al.*, 2004; Kosol-Ittikul *et al.*, 2008) and to make possible the study of springs with different gable bends, i.e. first, second, and third gable bends (Menghi *et al.*, 1999; Katona *et al.*, 2006). In the present study, a device for measuring forces and moments was used (Ferreira *et al.*, 2005).

The aim of this study was to evaluate and compare the results from numerical and experimental tests of an orthodontic retraction spring (Ferreira *et al.*, 2005). This study focused on the von Mises stress obtained with the FE method and force system resulting from activation of the spring in order to verify the maximum activation limit in which it maintains itself within the elastic range and, consequently, operational. No torque was measured.

Materials and methods

Numerical method

In order to evaluate the springs by means of the FE method, the computational software Ansys® (Swanson Analysis Systems, Houston, Pennsylvania, USA) was used. The basic idea of the method is to split the body or domain studied into subregions, the FEs. Based on that, the mathematical equations that govern the phenomenon studied for each subregion (FE) are prepared. The equations pertaining to each element are then joined, so that continuity is preserved, and one global equation is obtained to represent the entire body. In the static analysis of stress and strains, the equation (Cook *et al.*, 1998) that represents the body is given by

$$[K]\{u\} = \{F\}, \qquad (1)$$

where $[K]$ is the stiffness matrix, $\{u\}$ is the nodal displacement vector, and $\{F\}$ is the nodal force vector.

After finding the nodal displacements $\{u\}$ through the solution of the algebraic system shown in equation (1), the stresses and efforts on the the body may be evaluated. In this research, the spring was analysed using two-dimensional beam FEs, with two nodes per element and three degrees of freedom per node, that is, the spring was considered as plain. Figure 1 depicts the spring's dimensions, with representation of the wire section dimensions. The Young's modulus (E) obtained by mechanical tension tests was 69 GPa (10×10^6 psi) and the YS (σ_e) was equal to 1240 MPa (180×10^3 psi). As the displacements obtained were relatively large compared with the dimensions of the transverse section, the problem is non-linear. Thus, the matrix $[K]$ in equation (1) depends on the vector $\{u\}$, characterizing a non-linear system of equations. The activation was performed in increments of 1 mm in the horizontal direction, and considered maximum when, at any point, the spring material reached its yield stress limit and, consequently, suffered permanent deformation. At this point, the simulation process was terminated.

Samples

Twelve springs were manufactured using a titanium–molybdenum wire (Morelli, São Paulo, Brazil) with a 0.406 × 0.559 mm (0.016 × 0.022 inches) cross-section. The geometric configuration was characterized by having a central delta with an apical circumvolution with a radius of 1.5 mm and a one and a half-turn helix in its superior portion and gable bends in the horizontal extremities (Figure 1). The spring features were observed in relation to their reproducibility in a profile projection device (Projection Screen 560 × 460 mm, 0.5 per cent; working scale 0.1 mm; Henri Hauser SA, Bienne, Switzerland). Only the springs whose angular and linear dimensions were within the established tolerance limit were tested (Table 1). The geometric parameters were defined as alpha, beta, gama, and sigma angles.

Experimental method

It was established that Fx forces are caused by the activation of the spring in a horizontal direction, whereas Fy forces indicate vertical forces, which are perpendicular to Fx. Finally, Mz indicates the moment due to the inclinations in the extremities of the spring (sagittal plane). The springs were adapted for testing (A 1 mm right angle bend was placed in the alpha end to prevent sliding during activation
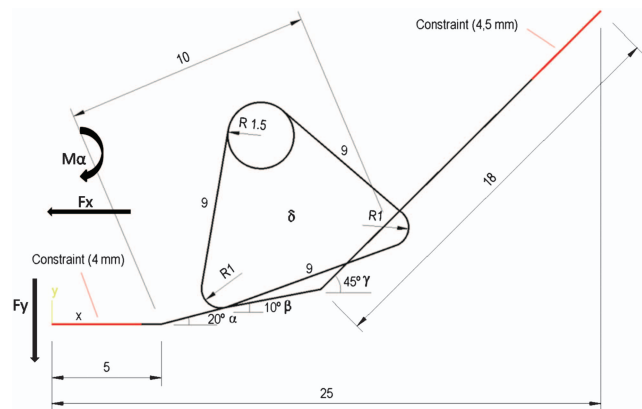

Figure 1 Delta spring dimensions. The arrows indicate the force system (vertical and horizontal forces and alpha moment).

Table 1 Spring dimensions and parameters.

Parameters	Tolerance	Dimensions
Radius (°)	±0.1	1.5
Height (mm)	±0.1	7.8
Angle δ (°)	±1	60
Angle α (°)	±1	20
Angle β (°)	±1	10
Angle γ (°)	±1	45
Length (mm)	±0.5	25
Cross-section (inches)	—	0.016 × 0.022

while the beta end was freely dislocated to activation) in a platform transducer. Each spring was activated from 0 to 6 mm. The transducer was calibrated by deadweight techniques. An analogue conditioner signal module feed by a 15 V source (Tektronix PS 280 DC Power Supply, Alpharetta, Georgia, USA) was attached to the transducer to amplify the variation of the signal emitted by the strain gauges after spring activation (Figure 2). The analogue

Figure 2 Transducer set. Platform (aluminum structure made up of a cross-shaped beam tied to its internal part, with 12 strain gauges; Power Source and Analogue Conditioner Signal Module.

electrical signals were converted to digital signals by means of a data acquisition board. The DASYLab® version 7.0—Data Acquisition System Laboratory (National Instruments Company, Austin, Texas, USA) software collected the signals from the data acquisition board.

Statistical analysis

Descriptive statistics for Fx are shown in Table 2. A one-way analysis of variance (ANOVA) for the experimental method was first performed in order to evaluate differences in Fx mean values according to activation. ANOVA showed a difference of $P \leq 0.01$(Table 3). The Games–Howell parametric multiple comparison test for heterogeneous variances was then used in order to identify the activations that were different (Table 4). This test highlighted a difference in all activations showing that mean forces increased and were significantly different for each activation level. The numerical method generates, for each activation, a mean value calculated by the software in a simultaneous way for the Fx parameter. Thus, there is no deviation. It is therefore necessary to compare the experimental method with the numerical method parameter. For each Fx activation in the numerical method, a comparison with the mean values found for experimental Fx was performed, at each activation level, by means of a Student's *t*-test.

Results

Stress–strain levels (numerical approach)

The stress level obtained with the numerical approach varied from 277 to 1273 MPa and from 1.4 to 8.1 mm of

Table 2 Descriptives statistics and means of force activation Fx.

Activation (mm)	n	Mean (gf)	Standard deviation	Standard error	95% confidence interval for mean		Minimum	Maximum
					Lower bound	Upper bound		
0	30	11.86	33.23	6.06	−0.549	24.27	−26.13	58.48
1	30	46.07	29.94	5.46	34.89	57.26	11.19	89.58
2	30	76.52	26.40	4.82	66.66	86.38	44.79	111.98
3	30	107.25	21.80	3.98	99.11	115.39	77.14	136.86
4	30	138.19	23.57	4.30	129.35	146.99	114.47	172.95
5	30	171.87	24.06	4.39	162.88	180.85	145.57	207.79
6	30	206.92	22.97	4.19	198.34	215.49	181.66	241.38

Table 3 One-way analysis of variance—tests of between-activations effect for the data—dependent variable force (Fx).

Source	Sum of squares	df	Mean square	F	P value	Observed power
Activation (mm)	865324.42	6	144220.73	208.74	0.00	1.00
Error	140250.98	203	690.89			
Corrected total	1005575.40	209				

activation, respectively (Table 5). Figure 3 shows the behaviour of the spring from von Mises stress analysis at 7 mm. At this activation, the springs were still below the elastic region (1082 MPa) and the superior part of the helical circumvolution showed the greater stress level.

Force levels

In the numerical test, a maximum activation of 8.1 mm was considered. Horizontal forces (Fx) varied from 0.1 N (10 gf) to 1.5 N (152 gf) for 1.4–6.1 mm activation. At maximum activation of 8.1 mm, the resulting force magnitude was about 2.2 N (224 gf). Vertical forces (Fy) showed constancy and were of low magnitude and could be disregarded. In the experimental test, a maximum

activation of 6 mm was considered. Horizontal forces (Fx) varied from 0.44 N (45 gf) at 1 mm to 2.02 N (206 gf) at 6 mm of activation. The spring gradient (spring rate) denotes the number of force–grams stored for each millimetre of activation. The spring rate in the present study was within the levels that are appropriate for clinical use (34 gf/mm). Figure 4a shows the behaviour of the experimental and numerical plots in relation to force versus activation and Figure 4b in relation to moment/force (M/F) ratio versus activation. There was a straight line from the plots even though the curves showed different angular coefficients. When analysing M/F ratio versus activation, more coincidence between plots was observed and M/F ratio decreased as activation

Table 4 Games–Howell parametric multiple comparisons test for heterogeneous variances; dependent variable: Fx.

Activation (mm)	n	Mean difference (I−J)	Standard error	P value	95% confidence interval	
					Lower bound	Upper bound
0	1	−34.21	8.16	0.00	−59.17	−9.26
	2	−64.66	7.74	0.00	−88.37	−40.94
	3	−95.39	7.25	0.00	−117.68	−73.10
	4	−126.33	7.43	0.00	−149.14	−103.52
	5	−160.01	7.49	0.00	−182.97	−137.05
	6	−195.05	7.37	0.00	−217.68	−172.43
1	0	34.21	8.16	0.00	9.26	9.17
	2	−30.44	7.28	0.00	−52.71	−8.16
	3	−61.17	6.76	0.00	−81.90	−40.45
	4	−92.11	6.95	0.00	−113.40	−70.82
	5	−125.79	7.01	0.00	−147.24	−104.34
	6	−160.84	6.89	0.00	−181.93	−139.74
2	0	64.66	7.74	0.00	40.94	88.37
	1	130.44	7.28	0.00	8.16	2.71
	3	−30.73	6.25	0.00	−49.85	−11.61
	4	−61.67	6.46	0.00	−81.41	−41.92
	5	−95.35	6.52	0.00	−115.27	−75.42
	6	−130.39	6.38	0.00	−149.92	−110.87
3	0	95.39	7.25	0.00	73.10	117.68
	1	61.17	6.76	0.00	40.45	81.90
	2	30.73	6.25	0.00	11.61	49.85
	4	−30.94	5.86	0.00	−48.85	−13.03
	5	−64.61	5.92	0.00	−82.73	−46.50
	6	−99.66	5.78	0.00	−117.32	−82.00
4	0	126.33	7.43	0.00	103.52	149.14
	1	92.11	6.95	0.00	70.82	113.40
	2	61.67	6.46	0.00	41.92	81.41
	3	30.94	5.86	0.00	13.031	48.85
	5	−33.67	6.14	0.00	−52.46	−14.89
	6	−68.72	6.00	0.00	−87.07	−50.37
5	0	160.01	7.49	0.00	137.05	182.97
	1	125.79	7.01	0.00	104.34	147.24
	2	95.35	6.52	0.00	75.42	115.27
	3	64.61	5.92	0.00	46.50	82.73
	4	33.67	6.14	0.00	14.89	52.46
	6	−35.04	6.07	0.00	−53.59	−16.49
6	0	195.05	7.37	0.00	172.43	217.68
	1	60.84	6.89	0.00	139.74	181.93
	2	130.39	6.38	0.00	110.87	149.92
	3	99.66	5.78	0.00	82.00	117.32
	4	68.72	6.00	0.00	50.37	87.07
	5	535.04	6.07	0.00	16.49	53.59

Table 5 Mean values of the force system for numerical test (finite element method).

| Activation (mm)	Fx (N)	Fx (gf)	Fy (N)	Mz (N mm)	Stress (MPa)	Mz/Fx (mm)
0	0.0	0.0	−0.02	1.57		Infinity
1.4	0.1	10.1	−0.02	2.11	277	21
1.8	0.2	20.3	−0.02	2.66		13
2.1	0.3	30.5	−0.02	3.20	335	10.6
2.5	0.4	40.7	−0.02	3.72		9.3
2.8	0.5	50.9	−0.02	4.23		8.4
3.2	0.6	61.1	−0.02	4.73	401	7.8
3.5	0.7	71.3	−0.02	5.21		7.4
3.8	0.8	81.5	−0.02	5.68		7.1
4.2	0.9	91.7	−0.02	6.14	528	6.8
4.5	1.0	101.9	−0.02	6.59		6.5
4.8	1.1	112.1	−0.03	7.02		6.3
5.1	1.2	122.3	−0.03	7.45	638	6.2
5.4	1.3	132.5	−0.03	7.86		6.0
5.7	1.4	142.7	−0.03	8.27		5.9
6.1	1.5	152.9	−0.03	8.66	773	5.7
6.4	1.6	163.0	−0.03	9.04		5.6
6.7	1.7	173.2	−0.03	9.41		5.5
7.0	1.8	183.4	−0.03	9.77	1082	5.4
7.3	1.9	193.6	−0.03	10.11		5.3
7.6	2.0	203.8	−0.03	10.45		5.2
7.8	2.1	214.0	−0.03	10.77		5.1
8.1	2.2	224.2	−0.03	11.08	1273	5.0
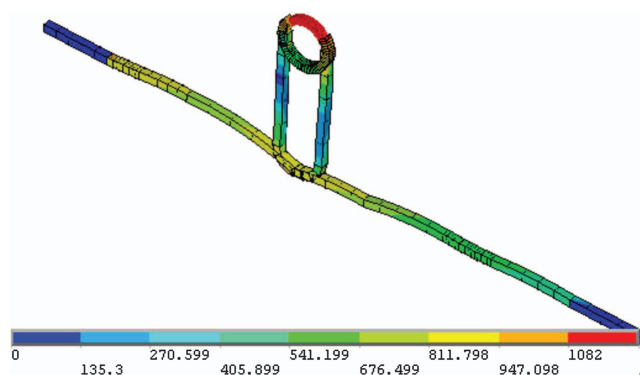
Figure 3 von Mises stress analysis of the behaviour of the delta spring. The critical area is near circumvolution. Yield strength is attained at 1240 MPa.

increased. The M/F ratio obtained with the numerical approach varied from 7.1 at 3.8 mm of activation to 13.0 at 1.8 mm of activation (Table 5), while M/F ratio from the experimental tests was 7.2 at 6 mm of activation increasing to 8.7 and 10.7 for 5 and 4 mm of activation, respectively (Table 6). The data may not exactly reflect clinical conditions, but the springs showed a tendency to produce controlled tooth movement if deactivated from 6 to 3 mm. The delta spring simulated an M/F ratio capable of producing sequential movement of controlled inclination followed by translation and, finally, by root correction during deactivation from 6 to 3 mm.
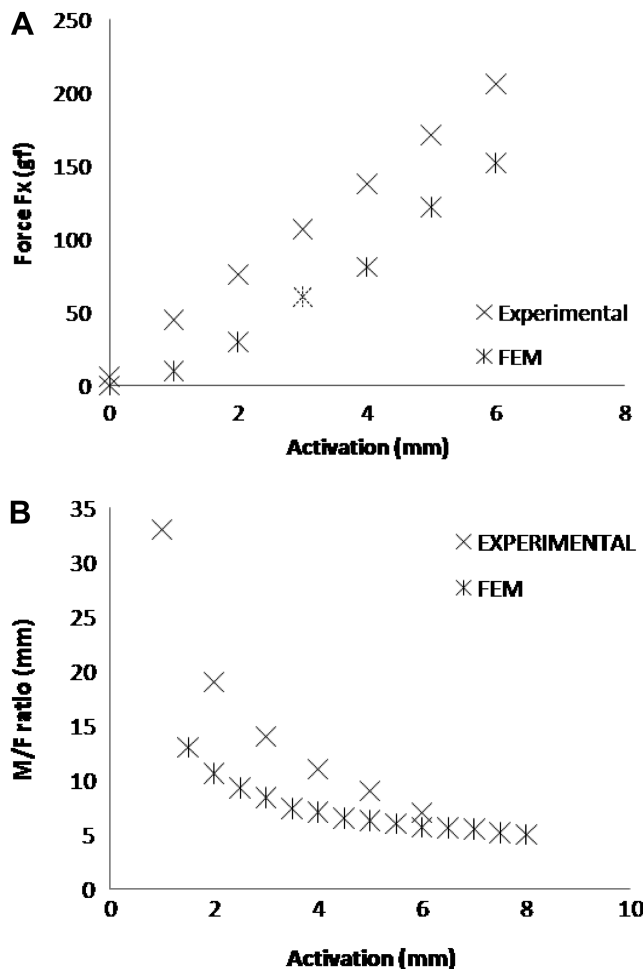

Figure 4 (A) Behaviour of experimental and analytical plots in relation to force versus activation up to 7 mm and (B) M/F ratio versus activation up to 7 mm.

Table 6 Force system from the experimental tests.

Activation (mm)	Fx (gf)	Fx (N)	Mz (gf mm)	Mz/Fx
0	6.3	0.05	1551	Infinity
1	45	0.44	1504	33
2	76	0.74	1515	19
3	107	1.04	1511	14
4	138	1.34	1488	10.7
5	171	1.67	1486	8.7
6	206	2.02	1501	7.2

Discussion

Clinicians hope to activate springs and visualize consequent tooth displacement in an efficient way. In general, this is undertaken by means of activation, observation, and fastening the springs as considered necessary. Even though spring behaviour is known, tooth anatomy and individual patient response are other variables that will influence tooth movement. Knowledge of a spring's

behaviour after application will minimize errors during activation. Although several studies (Yang and Baldwin, 1974; Raboud *et al.*, 1997; Siatkowski, 1997) applied the FE method, only a few studies are dedicated to verifying stress–strain behaviour in orthodontic springs. In the present research, the results show that the most critical regions for YS are located at the horizontal arms and at the spring apical helix (Figure 3). This means that the concentration of stress is located in the area close to the upper region, where the spring presents a circumvolution that serves as an imaginary axis around which the legs rotate. If there were no circumvolution, but just a semicircle, as in the case of simple vertical springs, a smaller stress level would surpass the YS of the material. Clinically, springs with circumvolutions are more appropriate for wider activations. One advantage is that as delta springs are activated their legs cross over each other providing greater stability and avoiding bucco-lingual inclination.

Ferreira *et al.* (2009), in a FE study, found for titanium–molybedneum asymmetric delta springs with a cross-section of 0.406 × 0.559 mm (0.016 × 0.022 inches) that critical stress (1108 MPa) was attained when the spring was activated 9 mm (in this case, the critical region is situated at the helix). In that study, a Young's modulus of 69 GPa and a YS of 1380 MPa was assumed. It is not necessary for such large activation but this result confirms that it is an efficient design to produce a long range of activation within a biomechanical force level. Concerning the stress results for 5.1 mm of activation, the critical region arises from the helix and horizontal anterior leg region but is under that of the elastic region (638 MPa). At 6.1 mm of activation, the total helix and part of the anterior leg regions showed the highest stress but still under elastic stress (773 MPa). This value is approximately the maximum safe clinical activation.

Several factors might influence spring design, such as the mechanical properties of the spring alloy, linear configuration, and cross-section. When comparing numerical and experimental methods, slight differences can occur. According to Figure 4a and 4b, these differences can be explained by the fact that the material property (Young's modulus) of the wire can be slightly different from that analysed with the FE method; crystallographic changes in metallurgic structure and residual stress are usually imposed in the spring's manufacturing process by cold working (plastic deformation); and the boundary conditions in the numerical simulation may not be exactly the same in all experiments, i.e. during simulation, the constraining points were immobile but in the experiment there was some mobility. A comparison between numerical and experimental methods is helpful to verify the limits of the analytical model and to determine that the models can be reproduced. In the current study, when comparing the methods in relation to force magnitude versus activation, it was evident that in the analytical model there was minimal difference in curve inclination but in the force–moment versus activation the

curves were similar, that is, for both methods there was concordance in relation to spring stiffness.

When the M/F ratio was analysed, agreement was found between the results obtained with both methods (Figure 4b). As soon as the spring was activated, the M/F relationship decreased (Tables 5 and 6). In this way, extrapolating clinically numerical results show a limited spectrum for controlled tooth movement when compared with experimental results. The literature shows that the M/F relationship decreases as the spring is activated and the present study confirms that (Raboud *et al.*, 1997; Burstone, 1982; Braun *et al.*, 1997; Siatkowski, 1997; Thiesen *et al.*, 2005). However, the works of Sander (2000) and Kum *et al.* (2004) have found constant values for the springs studied during deactivation from 6 mm to rest.

Conclusions

Delta springs produce a suitable force system compatible with sound biomechanics. Considering the values resulting from the spring's stress–strain behaviour, the force levels were adequate for high activations. Studies on orthodontic retraction springs should not only consider the force levels but also the stress–strain behaviour. If YS is surpassed during activation, the spring will work in a plastic region limiting its performance. Delta springs can be deactivated from 6 to 3 mm to produce canine retraction in a controlled movement and activated up to 7 mm to work safely within the elastic region.

Acknowledgement

We would like to thank Professor Sérgio A. Ignácio (Pontifical University of Paraná) for undertaking the statistical analysis.

References

Bourauel C, Drescher D, Ebling J, Broome D, Kanarachos A 1997 Superelastic nickel titanium alloy springs—an investigation of force systems. European Journal of Orthodontics 19: 491–500

Braun S, Sjursen R C, Legan L H 1997 On the management of extraction sites. American Journal of Orthodontics and Dentofacial Orthopedics 112: 645–655

Burstone C J 1966 The mechanics of the segmented arch techniques. Angle Orthodontist 36: 99–120

Burstone C J 1982 The segmented arch approach to space closure. American Journal of Orthodontics 82: 361–378

Burstone C J, Baldwin J J, Lawless D T 1961 The application of continuous forces to orthodontics. Angle Orthodontist 31: 1–14

Chen J, Markham D L, Katona T R 2000 Effects of T-loop geometry on its forces and moments. Angle Orthodontist 70: 48–51

Coimbra M E R, Penedo N D, Gouvêa J P, Elias C N, Araújo M T S, Coelho P G 2008 Mechanical testing and finite element analysis of orthodontic tear drop loop. American Journal of Orthodontics and Dentofacial Orthopedics 133: 188.e9–e13

Cook R D, Malkus D S, Plesha M E 1998 Concepts and applications of finite element analysis. John Wiley & Sons, New York

Ferreira M A 1999 The wire material and cross-section effect on double delta closing loops regarding load and spring rate magnitude: an *in vitro* study. American Journal of Orthodontics and Dentofacial Orthopedics 115: 275–282

Ferreira M A, Ignácio S A, Luersen M A, Borges P C 2004 Effects of the transversal section in the performance of a complex geometry planar retraction spring by the finite element method. Journal of Dental Clinics and Research 1: 25–30

Ferreira M A, Luersen M A, Borges P C 2009 Análise de tensões em uma alça de retração ortodôntica em delta por meio do método dos elementos finitos 3°. Encontro Nacional de Biomecânica. Vaz M A P, Piloto P A G, Reis Campos J C (eds). Bragança

Ferreira M A, Oliveira F T, Ignácio S A, Borges P C 2005 Experimental force definition system for a new orthodontic retraction spring. Angle Orthodontist 75: 334–343

Haskell B, Spencer S W A, Day M 1990 Auxiliary springs in continuous arch treatment: part I: an analytical study employing the finite element method. American Journal of Orthodontics and Dentofacial Orthopedics 98: 387–397

Katona T R, Yen P, Chen J 2006 The effect of first- and second order gable bends on force and moments generated by triangular loops. American Journal of Orthodontics and Dentofacial Orthopedics 124: 54–59

Koenig H A, Burstone C J 1989 Force systems from an ideal arch-large deflection considerations. Angle Orthodontist 59: 11–16

Koenig H A, Vanderby R, Solonche D J, Burstone C J 1980 Force system from orthodontic appliance: an analytical and experimental comparison. Transactions of the ASME 102: 294–298

Kosol-Ittikul P, Manosudprasit M, Godfrey K, Chartchaiwiwatana S, Piyasin S 2008 The analysis of load/deflection of four simple closing loop designs by using universal testing machine. Kaen Khon University Research Journal 2: 56–64

Kum M, Quick A, Hood J A, Herbison P 2004 Moment to force ratio characteristics of three Japanese NiTi and TMA closing loops. Australian Orthodontic Journal 20: 107–114

Manhartsberger C, Morton J Y, Burstone C J 1989 Space closure in adult patients using the segmented arch technique. Angle Orthodontist 59: 205–210

Menghi C, Planert J, Melsen B 1999 3-D experimental identification of force systems from orthodontic loops activated for first order corrections. Angle Orthodontist 69: 49–57

Ødegaard J, Meling T, Meling E 1996 The effects of loops on the torsional stiffnesses of rectangular wires: an *in vitro* study. American Journal of Orthodontics and Dentofacial Orthopedics 109: 496–505

Raboud D W, Faulkner M G, Lipsett A W, Haberstock D L 1997 Three dimensional effects in retraction appliance design. American Journal of Orthodontics and Dentofacial Orthopedics 112: 378–392

Rhee J, Chu Y, Row J 1997 A comparison between friction and frictionless mechanics with a new typodont simulation system. American Journal of Orthodontics and Dentofacial Orthopedics 119: 292–299

Rhee J, Chu Y, Row J 2002 A novel method for the three-dimensional (3-D) analysis of orthodontic tooth movement-calculation of rotation about and translation along the finite helical axis. Journal of Biomechanics 35: 45–51

Rinaldi T C, Johnson B E 1995 An analytical evaluation of a new spring design for segmented space closure. Angle Orthodontist 65: 187–198

Sander F G 2000 Biomechanical investigation of the hybrid retraction spring. Journal of Orofacial Orthopedics 61: 341–351

Siatkowski R E 1997 Continuous arch wire closing loop design, optimization and verification. Part I. American Journal of Orthodontics and Dentofacial Orthopedics 112: 393–402

Solonche D J, Burstone C J, Vanderby R 1977 A device for determining the mechanical behavior of orthodontic appliances. IEEE Transactions on Bio-medical Engineering 24: 538–539

Thiesen G, Rego M V N N, Menezes L M, Shimizu R H 2005 Force systems yielded by different designs of T-loop. Australian Orthodontic Journal 21: 103–110

Torstein R, Meling T R, Ødegaard J 1998 The effect of temperature on the elastic responses to longitudinal torsion of rectangular nickel titanium archwires. Angle Orthodontist 68: 357–368

Vanderby R, Burstone C J, Solonche D J, Ratches J A 1977 Experimentally determined force systems from vertically activated orthodontic loops. Angle Orthodontist 47: 272–279

Yang T Y, Baldwin J J 1974 Analysis of space closing springs in orthodontics. Journal of Biomechanics 7: 21–28